Optimized Measurement Location Planning for Interpolation-based Radio Environment Maps

Bastian Perner, Maximilian Lübke, and Norman Franchi
Institute for Smart Electronics and Systems
Friedrich-Alexander-Universität Erlangen-Nürnberg
Email: {bastian.perner, maximilian.luebke, norman.franchi}@fau.de

***Abstract*—Radio Environment Maps (REMs) play a crucial role in creating Electromagnetic (EM) situational awareness. This paper addresses the challenge of planning and optimizing measurement locations for REM construction, especially in time or resource-limited situations. Based on Optimal Experimental Design (OED), two measurement location planning strategies are derived from D-optimal and G-optimal design. In addition, the developed strategies are evaluated against baseline strategies and in terms of the impact of measurement density on the quality of REM construction. A measurement campaign at a music festival was carried out to collect real-world measurement data. The collected measurements provide a rural measurement dataset to evaluate different measurement location selection strategies. The results show that an optimized selection strategy can improve the accuracy of the REM construction by $6\,\mathrm{dB}$ on average compared to baseline methods.**

***Index Terms*—5G, Cognitive Radio, Electromagnetic Awareness, Measurement Planning, Optimal Experimental Design, Radio Environment Map, Spatial Spectrum Sensing**

I. Introduction

The evolution of wireless communication technologies, such as Cognitive Radio (CR) networks or the transition from fifth generation mobile network (5G) to sixth generation mobile network (6G), is leading to increasing demands, for example, in terms of adaptability to changing Electromagnetic (EM) conditions. In order to adapt the system to changing requirements, an awareness of the EM situation is required [1].

In this respect, Spatial Spectrum Sensing by using Radio Environment Maps (REMs) are a fundamental tool for creating such awareness. REMs provide a spatial representation of the Electromagnetic (EM) situation or the active radio signal characteristics, such as signal strength, interference power, or spectrum occupancy. This makes REMs a useful tool for spectrum management [2], opportunistic spectrum usage [3], or network optimization [4]. While there are indirect methods of generating REMs by estimating parameters such as location or transmit power [5], this work focuses on the direct approach, namely, interpolation-based REMs construction. Common examples of direct REM construction methods are Kriging, Inverse Distance Weighting (IDW), and Nearest Neighbor Interpolations (NNs) [6]. In this work, IDW is chosen because of its lower computational complexity compared to Kriging and it gives a continuous result in contrast to the NN approach.

Extensive spatially distributed measurements are required to generate accurate REMs. However, these are costly and time-consuming. The planning of measurement locations can mitigate those effects, e.g., by choosing a more efficient distribution of the measurement locations. It can, therefore, alleviate the degradation of REM construction with a reduced number of measurement locations. Various approaches exist that look at sensor placement strategies for interpolation algorithms. These methods, for example, are based on variogram gradients [7], PCA [8], or sensitivity matrices [9]. While [8], [9] require a-priori knowledge about propagation or channel characteristics, [7] is an update strategy to iteratively find the optimal placement of sensor nodes while making measurements.

In this paper, however, placement strategies solely rely on the spatial distribution of the measurement locations without any a-priori knowledge. In OED, the designs that, in this case, represent the distribution of the measurement locations are based on various optimality criteria. These optimality criteria are designed to optimize for objectives like minimizing uncertainty (D-optimal design) or maximizing robustness (G-optimal design) [10], [11]. Based on these principles, two strategies are derived and evaluated based on real-world measurements. The evaluation is based on comparing the derived strategies and two baseline strategies with respect to REM construction quality, a direct comparison between the two optimized strategies, and the effect of measurement density, defined as the number of measurements per area. The impact of measurement density gives insight into the planning of measurement campaigns, when assessing the number of needed measurement locations for a certain area size. The main contributions of the paper can be summarized as follows:

- Derivation of two measurement selection strategies based on OED: D-optimal and G-optimal design
- Evaluation of the derived measurement selection methods for REM construction based on OED optimality criteria
- Evaluation of measurement density impact on REMs

The paper is structured as follows. First, we present the overall scenario in section II. Section III describes the measurement setup and the available data set. Then we cover the methods, such as measurement selection strategies and interpolation method, in section IV. Section V presents the results. Finally, Section VI and Section VII discuss and conclude the work.

II. Scenario

This chapter gives a brief overview of the scenario and the notation. The initial situation is that there is a target area that needs to be monitored concerning the EM situation. Achieving a good REM with a limited number of measurement locations requires a good selection strategy. In the following, the notation used in this paper is introduced. Let:

- $\hat{A}$ be the target area to be monitored in terms of the EM situation.
- A be the set of regularly spaced rectangular grid points (interpolation grid) covering $\hat{A}$.
- $\Omega(A) = N_x \cdot N_y \cdot \Delta x \cdot \Delta y$ be the area covered by the interpolation grid A where N_x is the number of cells in x, N_y is the number of cells in y direction and Δx and Δy the respective step sizes. Here, we only consider 2D, but this can be extended to 3D by adding the z direction.
- $P \subset A$ be the set of available measurement locations.
- $S \subset P$ is a subset of N locations chosen for the interpolation-based REM construction, i.e., $|S| = N$.
- $\rho = \frac{|S|}{\Omega(A)}$ be the measurement density, defined as number of measurements per interpolation grid area $\Omega(A)$.

III. Measurements

A measurement campaign was conducted during a music festival in a crowded rural area shown in Fig. 1. A more detailed setup can be found in [3]. During that music festival,

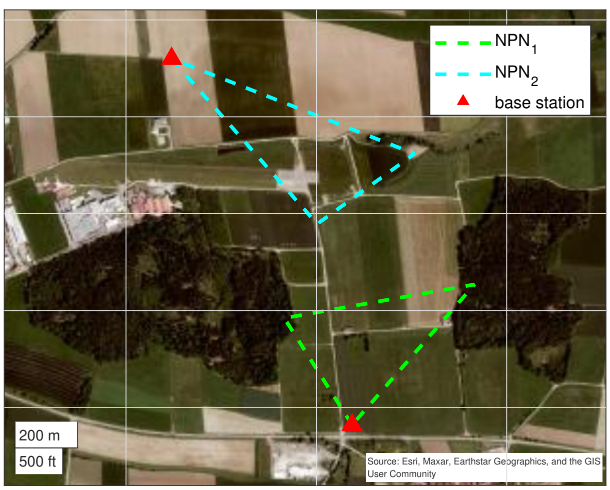

Fig. 1: Overview of the rural scenario of the measurement campaign, including the locations of two non-public network (NPN).

two 5G NPNs were deployed to evaluate and demonstrate the feasibility of spectrum sensing in a controlled scenario. One 5G NPN (NPN_1) was used as the primary base station while the other 5G NPN (NPN_2) served as an Emergency Communication System (ECS), providing communications to the Public Protection Disaster Relief (PPDR) personnel that was active at the festival. The schematic setup is shown in Fig. 1. The antennas of the 5G NPNs were oriented towards the infield of the festival site, as shown by the dashed areas in Fig. 1. Both 5G NPNs operated simultaneously in the same

Tab. 1: Hardware and Configuration

Device property	Details
Spectrum Analyzer	R&S TSMA6B
Frequency Range	$3.7\,\mathrm{GHz}$ to $3.8\,\mathrm{GHz}$
Sensitivity	$-160\,\mathrm{dB\,m}$

frequency range between $3.7\,\mathrm{GHz}$ to $3.8\,\mathrm{GHz}$ and used the available bandwidth of up to $100\,\mathrm{MHz}$. The equipment used

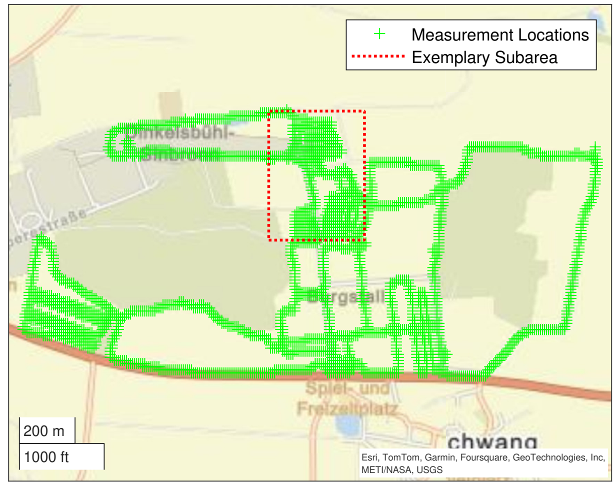

Fig. 2: Overview of available measurement locations and an example of a subarea used to evaluate different area sizes.

for collecting the measurement data and its configuration are listed in Tab. 1.

A. Measured Parameters

During the measurement campaign, the following parameters related to spectrum sensing were recorded:

- **SS-RSRP:** The Synchronization Signal Received Signal Reference Power (SS-RSRP) was measured to assess the signal strength of the deployed NPNs.
- **Power Spectral Density (PSD):** The power distribution across the frequency-domain was captured to analyze spectral characteristics of the signals.
- **Reference Position:** A corresponding GPS reference position was also determined for each measured value.

B. Overview of Measurement Collection and Processing

Fig. 2 shows the spatial coverage of the festival area. The total data collected covers recordings of approximately 10 hours. The recordings were taken over different days and merged into a common data set. After the measurement collection, the data was further processed. Measurements were aggregated to $10\,\mathrm{m} \times 10\,\mathrm{m}$ pixels covering the whole area, based on the corresponding reference position. Statistics were created on the summarized pixels, including minimum, maximum, mean, and median values. At locations or instances where the SS-RSRP was not detectable, a default value of $-160\,\mathrm{dB\,m}$ was assigned to ensure consistency across space in the dataset.

IV. Measurement Selection and Interpolation

We first derive two measurement selection strategies based on two respective OED optimality criteria. An algorithm was then developed for each of the strategies. These algorithms are so-called greedy algorithms, which may produce a sub-optimal solution. We then introduce the interpolation method and give an overview of the procedure from selection strategy to evaluating the REM construction.

A. Measurement Selection Strategy

The measurement selection strategies in this work are based on OED. Here, we use OED criteria to select a subset of design points that each optimize measurement selection for a statistical criterion.

For each point $p \in P$, let $x(p)$ denote its associated regression vector. Define the design matrix X for set S as:

$$X = \begin{bmatrix} x(p_1) & x(p_2) & \dots & x(p_N) \end{bmatrix}^T \tag{1}$$

and the corresponding Fisher information matrix:

$$M(S) = X^\top X. \tag{2}$$

The two OED criteria used in this work are D-optimality and G-optimality criteria [10], [11].

1) D-Optimality Criterion and MaxMin: D-optimality maximizes the determinant of the Fisher information matrix. It is defined as:

$$S_\text{D}^* = \arg \max_{S \subset P,\, |S|=N} \det(M(S)). \tag{3}$$

A higher determinant generally indicates that the design points are well spread out, as this maximizes the information. While we are aiming for interpolation instead of regression, the goal still is to find a well spread-out distribution of measurement points, which leads to the following:

$$S_\text{D}^* = \arg \max_{S \subset P,\, |S|=N} \min_{\substack{p_i,\, p_j \in S \\ i \neq j}} \|p_i - p_j\|_2. \tag{4}$$

In other words, we are looking for a subset of measurement points that maximizes the distance to the closest other measurement point. This leads to the first derived selection strategy and algorithm Algorithm 1:

Objective Select N points from a set $P = \{p_1, p_2, \dots, p_M\}$ such that the minimum pairwise distance between the selected points is maximized.

2) G-Optimality Criterion and MinMax: G-optimality minimizes the worst-case prediction variance over the design space. For a point p with regression vector $x(p)$, the prediction variance is proportional to

$$\text{Var} \propto x(p)^\top M(S)^{-1} x(p). \tag{5}$$

A G-optimal design minimizes the maximum variance:

$$S_\text{G}^* = \arg \min_{S \subset P,\, |S|=N} \max_{p \in P} x(p)^\top M(S)^{-1} x(p). \tag{6}$$

By minimizing the maximum prediction variance of a regression problem the worst-case interpolation error is minimized.

Algorithm 1 MaxMin Selection Strategy

Require: Potential measurement location set P and desired number of nodes N
Ensure: Selected set $S \subset P$ with $|S| = N$
  Initialize $S \leftarrow \{p_\text{first}\}$ {Choose an arbitrary starting point $p_\text{first} \in P$}
  while $|S| < N$ **do**
    for all $p \in P \setminus S$ **do**
      Compute $d(p) \leftarrow \min_{s \in S} \|p - s\|_2$
    end for
    $p_\text{new} \leftarrow \arg\max_{p \in P \setminus S} d(p)$
    $S \leftarrow S \cup \{p_\text{new}\}$
  end while

For interpolation this translates to the following statement: Every point that is estimated should be as close to a selected measurement point as possible, which leads to the following:

$$S_\text{G}^* = \arg \min_{S \subset P,\, |S|=N} \max_{a \in A} \min_{p_i \in S} \|p_i - a\|_2. \tag{7}$$

In other words, we try to select a subset of measurement points in order to minimize the distance to the subset for all points in A, which leads to the following strategy and algorithm 2:

Objective Select N points from $P = \{p_1, p_2, \dots, p_M\}$ such that the maximum distance of any point in A (the interpolation grid) to the closest selceted point is minimized.

Algorithm 2 MinMax Selection Strategy

Require: Candidate set P and desired number of nodes N
Ensure: Selected set $S \subset P$ with $|S| = N$
  Initialize $S \leftarrow \{p_\text{first}\}$ {Choose an arbitrary starting point $p_\text{first} \in P$}
  while $|S| < N$ **do**
    for all $p \in P \setminus S$ **do**
      Compute $d_{\min}(p) \leftarrow \min_{a \in A} \|p_i - a\|_2$
    end for
    $p_\text{new} \leftarrow \arg\max_{p \in P} d_{\min}(p)$
    $S \leftarrow S \cup \{p_\text{new}\}$
  end while

3) Baseline Strategies: For validation purposes, we also implemented two additional strategies for comparison. The first strategy aims to create a regular grid as options for measurement locations. As the available measurements shown in Fig. 2 do not follow a regular grid, the approach here is to take N measurement locations that are closest to the locations of the regular grid. We chose an equilateral triangular grid.

Objective (ClosestToGrid) Select N unique points from set P such that they are as close as possible to a regular grid.

The last strategy used in the evaluation is based on the random selection of N measurement locations from the available measurement locations within the target area A.

Objective (Random) Select N random unique points from set P.

B. REM Construction

IDW is an interpolation method known for its simplicity and low complexity. The idea behind this method is to attribute more weight to closer measurement locations [12]. In the context of REM, IDW is used to estimate the received power at all interpolation grid points $a \in A$.

C. Procedure and Evaluation Metrics

The processed data set was divided into subareas. One exemplary subarea is shown in Fig. 2. This subset of available measurement locations was then used to apply the different selection strategies, resulting in a set of N remaining measurement locations. This last set was then used to create a REM based on IDW. For evaluating the constructed REM, a baseline REM is created based on all available processed measurement data. The metric used to evaluate the different selection strategies is Mean Absolute Error (MAE) between the constructed REM (REM_c) and the baseline REM (REM_b), which is defined as follows:

$$\text{MAE}(A)\frac{1}{N_x N_y}\sum_{i=1}^{N_x}\sum_{j=1}^{N_y}|\text{REM}_b(x_i,y_j) - \text{REM}_c(x_i,y_j)| \quad (8)$$

V. Results

The following section first shows a comparison between the two derived OED-based strategies, MaxMin (Sec. IV-A1) and MinMax (Sec. IV-A2), and the two baseline strategies, namely Random and ClosestToGrid selection (Sec. IV-A3). After that, the effects of measurement density are investigated.

A. Comparison of Selection Strategies vs. Random Selection

We evaluated the performance of different sensor node selection strategies, namely MinMax, MaxMin, ClosestToGrid and Random. Figure 3 shows the REM construction error as a function of the number of locations N. It should be noted that Tab.2 shows the MAE averaged over different sections of the festival area. The size of these sections varies and is not fixed. Also, the measurement distribution within these sections varies highly. The two optimized strategies, MaxMin and MinMax, are close in performance shown in Fig. 3 and the results also show that the two optimized selection strategies outperform the two baseline strategies, Random and ClosestToGrid, when looking at the MAE of the REM construction error. The MAE of the REM construction for the MaxMin strategy is about $1\,\text{dB}$ lower than for the Random approach. Comparing ClosestToGrid and MaxMin, the MaxMin strategy outperforms the former by about $6\,\text{dB}$ in terms of MAE of REM construction. As stated in Tab. 2, both optimized strategies differ less than $0.5\,\text{dB}$ in REM construction accuracy across varying area sizes and a varying number of measurements.

B. Impact of Measurement Density

In the following, the impact of measurement density, defined as the number of measurement locations per target area, is evaluated for MinMax and MaxMin measurement selection strategies. Six different-sized rectangular areas were moved across the festival site, and REMs construction MAE were created for each target area respectively for a varying number of measurement locations as shown in Fig. 4, which also states the different sizes of the areas. All six show a similar tendency as the REM construction MAE decreases over a decreasing measurement density ρ regardless of measurement density. While the construction MAE for MinMax and MaxMin is nearly the same, for different area sizes, it can be seen that the reconstruction error is higher for bigger areas when having the same density. For example at a measurement density of $50\,\text{N}/\text{km}^2$, the MAE for a target area size of $750\,\text{m}\times 600\,\text{m}$ is at roughly $5\,\text{dB}$ compared to a construction error of about $4\,\text{dB}$ for a target area size $750\,\text{m}\times 400\,\text{m}$. Similar for a measurement density of $100\,\text{N}/\text{km}^2$, the construction error for a target area size of $500\,\text{m}\times 400\,\text{m}$ is about $2.5\,\text{dB}$ whereas for a target area size of $500\,\text{m}\times 200\,\text{m}$ is about $1.4\,\text{dB}$. These results will further be discussed in Sec. VI.

Tab. 2: Performance of selection strategies across different area sizes and different number of measurement locations N.

Strategy	**MAE** [dB]
ClosestToGrid	14.6
Random	10.1
MaxMin	8.7
MinMax	9.0

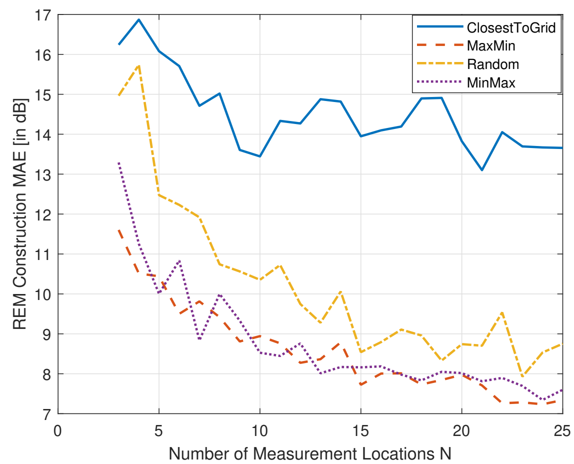

Fig. 3: Comparison of MAE of REM construction vs. number of measurement points for baseline selection and optimized strategies.

VI. Discussion

The results show that measurement location selection strategies have a significant effect on the quality of REM construction. By comparing the different strategies, namely the optimized MaxMin and MinMax approaches and the baseline strategies Random and ClosestToGrid, we have shown that the measurement location selection strategy can reduce the construction error of REM, even in the case of a limited number of measurement locations. The improved performance can be explained by the optimization goals of the derived strategies. The MaxMin strategy aims for the maximal spread

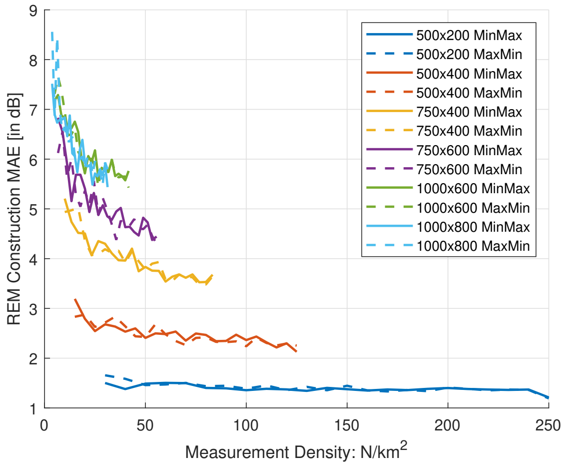

Fig. 4: Comparison of impact of measurement density for REM construction MAE based on MaxMin and MinMax selection strategies.

of measurement locations among the available locations. This results in a distribution of measurement locations covering a space as big as possible. Similar to that, the MinMax approach minimizes the distance of each interpolation grid point to a measurement location. This results in the most even distribution of measurement locations possible across the target area. Both strategies cover the target area in a better way for interpolation purposes compared to the Random and the ClosestToGrid strategy as in the two baseline strategies a local clustering of measurements can appear. Therefore, optimized selection results in a better interpolation outcome. While already outperforming baseline methods, further improvements can be expected if additional parameters such as terrain, environment, or existing domain knowledge are taken into account in the selection strategy.

Comparing the REM construction MAE for different area sizes, the expected patterns can be seen in Fig. 4, where the accuracy of the REM construction improves as the number of measurements used increases. While the density of measurements does not directly reflect the accuracy of the REM construction, as for larger areas, a higher density of measurements is required to achieve similar reconstruction accuracy results (see Fig. 4). This indicates that the number of measurements cannot be linked linearly to the target area. More in-depth investigations are necessary to work out the underlying relationships between measurement density and target area. Currently, the results indicate that there is no big difference in performance among the two optimized selection strategies, however a deeper comparison of the two strategies can show more insights into the differences, advantages, and disadvantages of both methods.

VII. Conclusion

This paper introduced two different strategies to select measurement locations for REM construction based on IDW interpolation to improve the quality of created REMs. Furthermore, a measurement campaign was conducted to collect real-world measurement data to show the feasibility of spatial spectrum sensing in PPDR missions. Using this data set, we showed an improvement in REM construction accuracy for both strategies based on OED optimality criteria compared to baseline selection strategies. These findings provide valuable input for measurement planning, resulting in better REM estimation, especially in situations with limited access to measurement locations or limited time to carry out measurements.

Acknowledgment

This work was funded by the German Federal Ministry of Digitalization and Transport (BMDV) within the project 5GOpportunity (grant number: 19OI22010B). The work contributes to the research within the 6G-Valley innovation cluster. The authors alone are responsible for the content of this paper.

References

[1] V. Shatov, M. Lübke, Y. Su, and N. Franchi, "On Integrated Cooperative Radio Sensing for Spatial Electromagnetic Analysis in 6G," in *2023 IEEE Future Networks World Forum (FNWF)*. Baltimore, MD, USA: IEEE, Nov. 2023, pp. 1–8. [Online]. Available: https://ieeexplore.ieee.org/document/10520344/

[2] J. Liu, F. Zhou, X. Liu, R. Ding, L. Yuan, and Q. Wu, "Data-and-semantic dual-driven spectrum map construction for 6g spectrum management," in *GLOBECOM 2024 - 2024 IEEE Global Communications Conference*, Cape Town, South Africa, 2024, pp. 139–144.

[3] K. Horbach, B. Perner, W. Rehmann, M. Kretschmer, M. Lübke, M. Rademacher, and N. Franchi, "Opportunistic 5g spectrum usage for nomadic ad-hoc emergency communication," in *2024 IEEE Future Networks World Forum (FNWF)*, Dubai, United Arab Emirates, Oct. 2024, pp. 698–703.

[4] A. C. Suarez Rodriguez, N. Haider, Y. He, and E. Dutkiewicz, "Network optimisation in 5g networks: A radio environment map approach," *IEEE Transactions on Vehicular Technology*, vol. 69, no. 10, pp. 12 043–12 057, 2020.

[5] S. Alfattani and A. Yongacoglu, "Indirect methods for constructing radio environment map," in *2018 IEEE Canadian Conference on Electrical Computer Engineering (CCECE)*, Quebec, QC, Canada, 2018, pp. 1–5.

[6] M. Pesko, T. Javornik, A. Kosir, M. Štular, and M. Mohorcic, "Radio environment maps: The survey of construction methods," *KSII Transactions on Internet and Information Systems*, vol. 8, 2014.

[7] Y. Nakamura, M. Ito, and K. Sezaki, "Planning Placement of Distributed Sensor Nodes to Achieve Efficient Measurement," in *Distributed, Ambient and Pervasive Interactions: Understanding Humans*, N. Streitz and S. Konomi, Eds. Cham: Springer International Publishing, 2018, vol. 10921, pp. 103–113, series Title: Lecture Notes in Computer Science.

[8] L. Wei, X. Mo, S. Sun, and L. Gui, "Spatial sampling points selection for 3d rem construciton," in *2022 IEEE 8th International Conference on Computer and Communications (ICCC)*, Chengdu, China, 2022, pp. 2123–2127.

[9] S. Boatwright, M. Romano, S. Mounce, K. Woodward, and J. Boxall, "Optimal sensor placement and leak/burst localisation in a water distribution system using spatially-constrained inverse-distance weighted interpolation," in *Proceedings of the 13th international conference on hydroinformatics*, Palermo, Italy, 2018, pp. 1–6.

[10] A. C. Atkinson, A. N. Donev, and R. D. Tobias, *Optimum Experimental Designs, with SAS*. Oxford University Press, 05 2007.

[11] R. C. S. John and N. R. Draper, "D-optimality for regression designs: A review," *Technometrics*, vol. 17, pp. 15–23, 1975. [Online]. Available: https://api.semanticscholar.org/CorpusID:120997070

[12] J. Ojaniemi, J. Kalliovaara, A. Alam, J. Poikonen, and R. Wichman, "Optimal field measurement design for radio environment mapping," in *2013 47th Annual Conference on Information Sciences and Systems (CISS)*. Baltimore, MD, USA: IEEE, Mar. 2013, pp. 1–6. [Online]. Available: https://ieeexplore.ieee.org/document/6552334/